

# Effect of Insertion Devices in SPEAR 3<sup>1</sup>

J. Corbett and Y. Nosochkov

Stanford Linear Accelerator Center, Stanford University, Stanford, CA 94309

## Abstract

The SPEAR 3 upgrade lattice will provide much reduced beam emittance to increase the brightness of synchrotron radiation beams from wigglers and undulators. Seven existing insertion devices will be used in the lattice. In this paper we review the wiggler parameters, outline the wiggler compensation scheme, and evaluate wiggler effect on the optics and dynamic aperture.

*Presented at the 1999 IEEE Particle Accelerator Conference (PAC99)  
New York City, New York, March 29 – April 2, 1999*

---

<sup>1</sup>Work supported by Department of Energy contract DE-AC03-76SF00515.

# EFFECT OF INSERTION DEVICES IN SPEAR 3<sup>†</sup>

J. Corbett<sup>‡</sup> and Y. Nosochkov

Stanford Linear Accelerator Center, Stanford University, Stanford, CA 94309

## Abstract

The SPEAR 3 upgrade lattice will provide much reduced beam emittance to increase the brightness of synchrotron radiation beams from wigglers and undulators. Seven existing insertion devices will be used in the lattice. In this paper we review the wiggler parameters, outline the wiggler compensation scheme, and evaluate wiggler effect on the optics and dynamic aperture.

## 1 INTRODUCTION

Many of the drift sections in SPEAR 3 will contain wigglers or undulators. In the present machine, there are 7 insertion devices (ID). In this paper, we review the magnetic parameters for each of these ID's, estimate linear and higher order wiggler effects, evaluate radiation effects, and discuss correction of wiggler focusing using quadrupole trim windings. Tracking results show that dynamic aperture reduction due to wiggler effects is modest. All optics calculations were done with the MAD code [1], and the tracking simulations with the LEGO code [2].

## 2 WIGGLER PARAMETERS, EFFECTS AND MODELING

In SPEAR 3, the horizontally deflecting ID's reside in dispersion free straights where the unperturbed  $\beta$  functions are  $\beta_x/\beta_y = 10.1/4.8$  m. The magnetic field parameters for each ID are given in Table 1, where  $N$  is the number of periods,  $\lambda$  the period length,  $B_o$  the peak field.<sup>1</sup> Future devices are likely to be  $\sim 10$ -period wigglers similar to Beamlines 9 and 11. These devices will replace the wigglers on Beamlines 4 and 7 or illuminate new beam lines.

The main optical effects of the wigglers on the SPEAR 3 lattice are also summarized in Table 1. The parameter definitions and relevant formulas are listed below:

Bend radius	$\rho_o(m) = 3.3356 \frac{E(GeV)}{B_o(T)}$
Wiggler parameter	$K = 93.44 B_o(T) \lambda(m)$
Integrated focusing [3]	$\int k_y ds = \frac{N\lambda}{2\rho_o^2}$
Linear tune shift	$\Delta Q_y = \frac{\beta_y}{4\pi} \int k_y ds$
Maximum $\beta$ -beat	$\frac{\Delta\beta_y}{\beta_y} = \frac{\beta_y \int k_y ds}{2\sin 2\pi Q_y}$
Amplitude dependent tune shift [4]	$\Delta Q_y^{oct} = \epsilon_y \frac{\pi N \beta_y^2}{4\lambda \rho_o^2} \left[ 1 + \frac{2}{3} \left( \frac{N\lambda}{2\beta_y} \right)^2 + \frac{1}{5} \left( \frac{N\lambda}{2\beta_y} \right)^4 \right]$

<sup>†</sup> Work supported by the Department of Energy Contract DE-AC03-76SF00515.

<sup>‡</sup> E-mail: corbett@slac.stanford.edu.

<sup>1</sup> Beamline 5 can use five separate devices: (1)  $N=10$ ,  $\lambda=0.18$ , (2)  $N=15$ ,  $\lambda=0.12$ , (3)  $N=24$ ,  $\lambda=0.07$ , (4)  $N=30$ ,  $\lambda=0.06$ , and (5) elliptically polarized undulator (EPU). Here, we chose the  $N=10$ ,  $\lambda=0.18$  wiggler.

Table 1: Wiggler parameters and main optics effects.

Beamline	4,7	5	6	9	10	11
$N$	4	10	27	8	15	13
$\lambda$ (cm)	45	18	7	26	13	17.4
$B_o$ (T)	1.8	0.9	1.3	1.93	1.45	1.98
$\rho_o$ (m)	5.56	11.12	7.70	5.18	6.90	5.05
$K$	75.7	15.1	8.5	46.9	17.6	32.2
$\int k_y ds$ ( $m^{-1}$ )	.029	.007	.016	.039	.021	.044
$\Delta Q_y$	.011	.003	.006	.015	.008	.017
$\Delta\beta_y/\beta_y$ (%)	7.0	1.8	3.9	9.4	5.0	10.7
$\Delta Q_y^{oct}$ [ $10^{-4}$ ]	0.4	0.6	9.1	1.6	3.4	4.1

where  $Q_y=5.23$  is the vertical betatron tune,  $\epsilon_y$  the vertical emittance, and  $E=3$  GeV the beam energy.

For a flat horizontal wiggler the field components can be expressed as [5]:

$$B_y = B_o \cosh(ky) \cos(kz), \quad (1)$$

$$B_z = -B_o \sinh(ky) \sin(kz), \quad (2)$$

where  $k = 2\pi/\lambda$ ,  $y$  and  $z$  are the vertical and longitudinal coordinates, and  $z=0$  the center of a pole. The integral of the  $B_y$  field (Eqn. 1) with respect to the reference trajectory vanishes over each wiggler period. This leads to self compensation of the optics effects. For instance, the horizontal orbit and dispersion generated by  $B_y$  are fully localized within each period. The amplitude of the orbit and dispersion is proportional to  $\lambda^2 B_o$ , and the increase in beam path length is proportional to  $\lambda^3 B_o^2 N$ . Hence, the largest orbit oscillations are produced in the wigglers with the longest poles. The total increase of the path length for all 7 wigglers is 191  $\mu$ m.

Taking into account the horizontal orbit oscillations of the beam, the  $B_z$  field (Eqn. 2) can be decomposed into longitudinal and horizontal components on the beam orbit. Although the integral of the longitudinal component vanishes over each period, one can find a non-zero integral of the field horizontal to the beam trajectory [3]:

$$\int_o^{N\lambda} B_x dz = -\frac{N\lambda B_o^2}{2B\rho} \left( y + \frac{2}{3} k^2 y^3 + \frac{2}{15} k^4 y^5 + \dots \right), \quad (3)$$

where label  $\tilde{x}$  refers to the local horizontal axis with respect to the oscillating beam orbit.

The first term in Eqn. 3 ( $\propto y$ ) is similar to the vertical gradient in quadrupoles and thus results in vertical focusing, namely the vertical tune shift  $\Delta Q_y$  and vertical betatron beat  $\Delta\beta_y/\beta_y$ . The total linear tune shift is  $\Delta Q_y=0.071$  for all 7 wigglers. The pattern of the  $\beta$ -beat depends on the distribution of wigglers in the ring. The  $\sim 90^\circ$  vertical phase advance per cell helps to minimize beta perturbations

from a pair of wigglers if they are located on either side of the same cell. All 7 wigglers generate about  $\pm 25\%$  vertical  $\beta$ -beat in the ring without correction.

The first non-linear wiggler effect comes from the second term in Eqn. 3 ( $\propto y^3$ ). This octupole-like field generates quadratically increasing vertical tune shift with  $y$ -amplitude. For devices of similar length ( $N\lambda$ ) the effect is proportional to  $1/\lambda^2$ . In Table 1, this tune shift was evaluated for the maximum vertical emittance ( $\epsilon_y=7.5$  mm-mrad) defined by the smallest vacuum chambers at Beamlines 6 and 11 ( $y=6$  mm,  $\beta_y=4.8$  m). The maximum total tune shift for 7 wigglers is  $\Delta Q_y^{oct}=0.002$ . This value is significantly smaller than the amplitude dependent tune shift caused by the sextupoles and was considered acceptable. Tracking simulations with wiggler effects confirm that the vertical dynamic aperture stays well outside the physical wiggler aperture.

For optics calculations, each wiggler pole was simulated by a shorter pole with constant vertical field and with gaps between the poles [3]. In this model, the pole field,  $B_p = B_o \pi/4$ , and pole length,  $L_p = 4\lambda/\pi^2$ , were set to produce the same bending and focusing effect as the actual wiggler field. Therefore, the model yields the correct linear tune shift,  $\beta$ -beat, and the net orbit and dispersion. For tracking studies, higher order multipole fields were added to simulate the effects of non-linear wiggler fields on dynamic aperture.

### 3 RADIATION EFFECTS

Synchrotron radiation and quantum excitation in wigglers increase the beam energy loss and change the equilibrium emittance and the beam energy spread. For a single ID, the relative increase in energy loss per turn is [6]:

$$\frac{U - U_o}{U_o} = \frac{N\lambda\rho_b}{4\pi\rho_o^2}, \quad (4)$$

where  $\rho_b=7.86$  m is the bend radius in the main dipoles, and  $U_o=913$  keV/turn (without ID's). The energy loss with all 7 wigglers at full field increases by 23% to 1124 keV/turn. The total radiated wiggler power is 225 kW from a 200 mA beam.

The relative change in the beam energy spread due to each ID is given by [6]:

$$\left(\frac{\sigma_E}{\sigma_E^o}\right)^2 = \left[1 + \frac{2N\lambda\rho_b^2}{3\pi^2\rho_o^3}\right] \left[1 + \frac{N\lambda\rho_b}{4\pi\rho_o^2}\right]. \quad (5)$$

With 7 wigglers at full field, the net energy spread on the beam increases by only 1.6%, from  $\sigma_E^o/E=0.097\%$  to

Table 2: Change in energy loss and energy spread due to wigglers.

Beamline	4,7	5	6	9	10	11
$\frac{U-U_o}{U_o}(\%)$	3.64	0.91	1.99	4.84	2.56	5.54
$\frac{\sigma_E-\sigma_E^o}{\sigma_E^o}(\%)$	0.35	-0.18	-0.13	0.66	-0.04	0.84

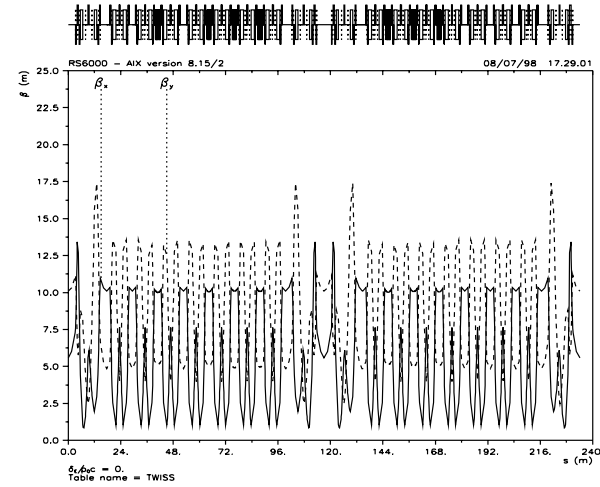


Figure 1: SPEAR 3  $\beta$  functions with 7 wigglers (black boxes on the top) after correction.

0.0986%. The effects of individual ID's are listed in Table 2. Emittance calculations show that 7 wigglers reduce the horizontal emittance from 18.2 nm-rad to 15.3 nm-rad.

### 4 OPTICS COMPENSATION

The wiggler focusing from 7 wigglers at full field generates  $\pm 25\%$  vertical  $\beta$ -beat and a linear vertical tune shift of 0.071. This distortion breaks the periodicity of the  $\beta$ -functions and phase advance between sextupoles, which could lead to stronger sextupole resonances and reduced dynamic aperture.

Several options are possible to correct the wiggler focusing. The preferred scheme is to locally compensate the distortion of  $\beta$ -functions and phase advance with four QF and four QD independent quadrupole trims located to either side of each ID. With this correction, the phase advance stays identical in all cells, the global tune adjustment is not necessary and the distortion of lattice functions at sextupoles is minimal. The required independent quadrupole trims are less than 10%. This correction scheme has been designed into the SPEAR 3 lattice and was used in tracking studies described in the following section. The SPEAR 3  $\beta$  functions after correction of 7 wigglers are shown in Fig. 1.

### 5 EFFECT ON DYNAMIC APERTURE

Effects of IDs on dynamic aperture arise from reduced symmetry and lattice periodicity, distortion of  $\beta$ -functions and betatron phase, non-linear wiggler fields, wiggler field errors and misalignment. In tracking simulations, we studied the following effects of wigglers on dynamic aperture:

- Linear wiggler focusing,
- Effect of systematic multipole field errors in wigglers,
- Effect of intrinsic non-linear wiggler field.

Without correction of the wiggler focusing, the vertical dynamic aperture reduces by about 20% with all wigglers

Table 3: Multipole fit to the measured systematic multipole field error in the wiggler on Beamline 11 ( $G/cm^{n-2}$ ).

$n$	1	2	3	4	5	6
$b_n L$	20.3	-6.49	-15.5	-37.2	5.96	33.2
$a_n L$	19.4	17.9	-35.4	26.4	3.64	-65.0

$n$	7	8	9	10	11	12
$b_n L$	2.73	-7.40	-1.05	0.457	0.079	0.001
$a_n L$	13.9	33.3	-3.55	-5.57	0.227	0.297

active. With corrected wiggler focusing, linear wiggler effects alone do not reduce the aperture.

The study of wiggler multipole errors was based on measured systematic field errors in the wiggler on Beamline 11. A numerical multipole fit to the measured data was performed and the results for the integral of normal and skew systematic multipole field are shown in Table 3, where ‘ $n$ ’ is the multipole order starting with dipole,  $L = N\lambda$ , and  $a_n, b_n$  are the skew and normal field coefficients defined as

$$B_y + iB_x = \sum_n (b_n + ia_n)(x + iy)^{n-1}. \quad (6)$$

The effect of 7 wigglers on dynamic aperture is shown in Fig. 2, with the aperture calculated at the ID locations ( $\beta_x/\beta_y = 10.1/4.8$  m) for machine simulations with all errors in the ring magnets. Without multipole errors in the wigglers but with corrected wiggler focusing, the aperture is not affected. With the systematic multipole errors included in the 7 wigglers, the dynamic aperture reduction is about 10% (2 mm).

The wiggler-intrinsic high order terms (Eqn. 3) were not included in the previous simulation, but can further reduce the dynamic aperture. This field does not have the usual form of  $(x-y)$  multipole expansion normally used in lattice codes. To accurately study the effect of the octupole-like and higher order terms in Eqn. 3, one needs a symplectic model of this field. We used an approximation to evaluate the main effect of these terms. Since the non-linear  $B_x$  field generates kicks only in  $y$ -plane, the effect on dynamic aperture is expected to be mostly in the vertical plane, as it was observed in simulations for other machines [6].

One can notice that the  $B_x$  field can be reproduced at  $x=0$  by the normal field of Eqn. 6 ( $a_n=0$ ). Using this approach, we used normal systematic multipoles in the form of  $B_y + iB_x = \sum b_n(x + iy)^{n-1}$  to produce the non-linear terms of the wiggler field  $B_x$  on the vertical axis (Eqn. 3), and performed tracking to evaluate vertical aperture near  $x=0$ . Simulation of the octupole-like and dodecapole-like ( $\propto y^5$ ) fields with 7 wigglers showed only modest reduction of vertical dynamic aperture, from 11 mm to 8-9 mm. This aperture still remains well outside the 6 mm wiggler physical aperture.

## 6 SUMMARY

Tracking simulations with 7 wigglers in SPEAR 3 predict small impact on dynamic aperture when linear optics ef-

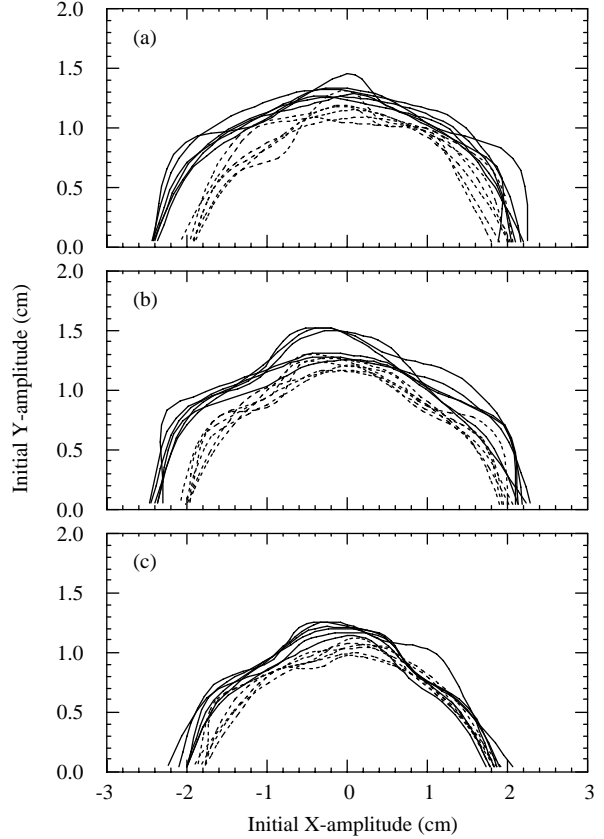


Figure 2: Dynamic aperture for  $\delta=0$  (solid) and 3% (dash) off-momentum oscillations and 6 seeds of random machine errors: (a) no wigglers, (b) 7 wigglers with corrected focusing but w/o errors, (c) 7 wigglers with corrected focusing and with systematic multipole errors.

fects are locally compensated with individually controlled quadrupole magnets. The 18 mm horizontal dynamic aperture is sufficient for 10 mm injection oscillations and long Touschek lifetime, and the vertical aperture remains well outside the 6 mm wiggler physical aperture. With all wigglers active, the increase in energy spread is negligible ( $<2\%$ ), and the beam horizontal emittance decreases to about 15.3 nm·rad at 3 GeV.

## 7 ACKNOWLEDGEMENTS

We would like to thank M. Cornacchia, H. Wiedemann and B. Hettel for useful discussions, suggestions and guidance.

## 8 REFERENCES

- [1] H. Grote, F. C. Iselin, CERN/SL/90-13 (AP) Rev.4 (1994).
- [2] Y. Cai *et al.*, SLAC-PUB-7642 (1997).
- [3] H. Wiedemann, “Particle Accelerator Physics II,” Springer-Verlag, Berlin, Heidelberg (1995).
- [4] L. Smith, LBL-ESG Tech. Note-24 (1986).
- [5] K. Halbach, *NIM*, A187, p. 109 (1981).
- [6] A. Ropert, CERN 90-03, p. 142 (1990).